A Composite Phase Plane for Tubular Reactor Stability Studies

FRANK S. WANG

University of Illinois, Urbana, Illinois

and

D. D. PERLMUTTER

University of Pennsylvania, Philadelphia, Pennsylvania

A composite phase plane is introduced in order to describe geometrically the transients of a distributed parameter system with only one physical dimension. Its intrinsic features are discussed and compared with those of the ordinary phase plane. For the plug-flow tubular reactor an equivalence is established between bounds on the reactor transients and the confinement of their projections on the composite phase plane. A constrained integration method is developed which enables one to find a region of stability for an adiabatic reactor, and a related technique is demonstrated for a nonadiabatic case. A hypothetical reactor system is analyzed numerically to illustrate the application.

The geometric arguments that accompany a phase plane description of a dynamic system are well established in the fields of control and reactor design, especially as they relate to transient bounds and stability relations. It is interesting to note however that the various developments focus either exclusively on lumped-parameter continuous stirred-tank reactor models or steady state tubular reactor behavior.

It is the purpose of this paper to show that the well-known substantial derivative transformation may be used to define a composite phase plane which is useful in the analysis of a plug-flow tubular reactor and retains much of the geometric advantages of the familiar phase plane of a lumped-parameter system. The analogous points of the two are by no means self-evident, and the following will focus on finding the significant differences and justifying those parallels that do exist.

Recall that the phase plane for a continuous stirred-tank reactor (CSTR) system (*2, 4, 7, 8, 11, 13*) is ordinarily the concentration vs. temperature plane. When the coordinates are translated such that the origin is at the steady state (point) of interest, the phase plane will be in terms of disturbed concentration and temperature $(\hat{C}, \hat{\eta})$. Since the steady state concentration and temperature in a tubular reactor are varying along the reactor, the steady state profile is a curve stretching from $x = 0$ to $x = L$ in (C, η, x) space. At each x location a phase plane in terms of $\hat{C}$ and $\hat{\eta}$ can be formed from known values of C_s and η_s at that point. As shown in Figure 1, every one of these phase planes has its origin on the steady state profile and is perpendicular to the x axis.

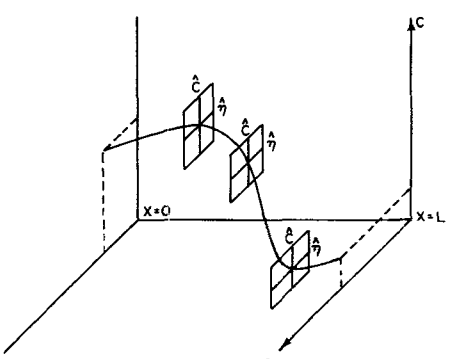

Fig. 1. A series of ordinary phase planes along a steady state curve in the space (C, η, x).

A composite phase plane (CPP) may be defined in terms of $\hat{C}$ and $\hat{\eta}$ as a projection of the set of ordinary

phase planes in the x direction but along the steady state profile. The ordinary phase plane of a CSTR system may in a sense be considered as a special case of the composite phase plane; however, the latter has its origin corresponding to a steady state profile and the former to a single steady state point. A typical composite phase plane is shown in Figure 2.

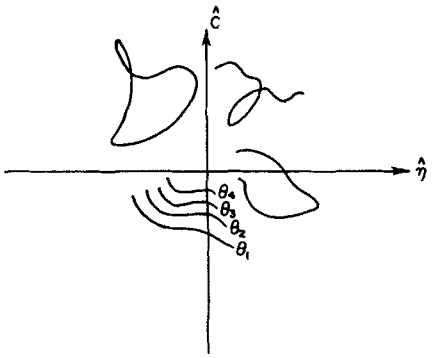

Fig. 2. A composite phase plane with projections of typical transient curves in the space (C, η, x).

The state of a CSTR at any moment can be represented by a unique point in the ordinary phase plane. Its transient is the locus travelled by that point as time goes on. Such trajectories do not cross each other or intersect themselves, except in the case of limit cycles or at singular points, but depend only on initial conditions. In contrast, the state of a tubular reactor is a profile in $(\hat{C}, \hat{\eta}, x)$ space, whose projection on the CPP requires representation by the continuous variation with respect to time of the projected curve. The transient curve on the CPP may vary its shape, length, and position, depending entirely on the details of a particular system.

In the process of projection, the x position of every point on the transient curve is ignored. As a result the projected curves can intersect themselves or form closed contours, if there are several points on a transient curve possessing the same $\hat{C}$ and $\hat{\eta}$ at different positions along the x axis. This also points out that although each transient curve gives only one projected curve on the CPP, a given curve on the CPP may correspond to more than one transient curve in (C, η, x) space. Several arbitrary projected curves on CPP are shown in Figure 2. Since trajectories in the phase plane represent unique transients of a CSTR system, interpolation between trajectories is valid, and a finite number of trajectories on the phase plane are sufficient to show the dynamics of a CSTR system (*12*). This convenient feature does not necessarily attach to the composite phase plane because of the nonunique correspondence between a projected and a transient curve. Hence the calculation of a few transient profiles whose projections cover a region in the CPP is not sufficient to establish the dynamics of a tubular reactor.

SYSTEM EQUATIONS

A tubular reactor is said to operate under plug-flow conditions, if axial mixing and diffusion and radial temperature and concentration gradients are negligible. These two assumptions normally also imply a flat velocity profile across the reactor section. Velocity and all other physical constants of the fluid are treated as constant throughout the reactor. In the case of a nonadiabatic reactor, constant wall temperature and heat transfer coefficient are assumed.

The transients of such a plug-flow tubular reactor (PFTR) can be described by the following pair of first-order, quasilinear partial differential equations (PDE) and end conditions:

$$\partial C/\partial\theta = -v\,(\partial C/\partial x) - R \tag{1a}$$

$$\rho C_p \partial T/\partial\theta = -\rho C_p v\,(\partial T/\partial x) + \Delta HR - K\,(T - T_w)\,A_r \tag{1b}$$

$$C(0, x) = \phi_1(x);\ T(0, x) = \phi_2(x) \tag{1c}$$

$$C(\theta, 0) = C_o;\ T(\theta, 0) = T_o \tag{1d}$$

The boundary conditions deserve particular attention in analyzing the stability of a distributed parameter system.

By letting $\eta = (C_p\rho T/\Delta H)$ and $G = KA_r/\rho C_p$, Equation (1*b*) is normalized to

$$\partial\eta/\partial\theta = -v(\partial\eta/\partial x) + R - G(\eta - \eta_w) \tag{2}$$

and the steady state system is governed by

$$v(dC_s/dx) = -R_s \tag{3a}$$

$$v(d\eta_s/dx) = R_s - G(\eta_s - \eta_w) \tag{3b}$$

$$C_s(0) = C_{so};\ \eta_s(0) = \eta_{so} \tag{3c}$$

For any fixed inlet conditions, solutions of Equations (3*a*) and (3*b*) give a pair of steady state concentration and temperature profiles $C_s(x)$ and $\eta_s(x)$ with respect to which disturbance variables can be defined as

$$\hat{C} = C - C_s \text{ and } \hat{\eta} = \eta - \eta_s$$

Then

$$\partial\hat{C}/\partial\theta = -v(\partial\hat{C}/\partial x) - \hat{R} \tag{4a}$$

$$\partial\hat{\eta}/\partial\theta = -v(\partial\hat{\eta}/\partial x) + \hat{R} - G\hat{\eta} \tag{4b}$$

where $\hat{R} = R - R_s$

It should be noted that $\hat{R}$ can be treated as a function of $\hat{C}$ and $\hat{\eta}$ with two parameters C_s and η_s, the steady state profiles. The trivial solution $\hat{C} = 0$, $\hat{\eta} = 0$ represents these steady state profiles. The stability of a given steady state is investigated through Equations (4). At the same time Equations (1*c*) and (1*d*) suggest that disturbances in the form of initial profiles as well as perturbed inlet conditions should be expected.

SUBSTANTIAL DERIVATIVE TRANSFORMATION

If a substantial derivative is defined in the usual well-known manner (*5*), Equations (4) become

$$D\hat{C}/D\tau = -\hat{R} \tag{5a}$$

$$D\hat{\eta}/D\tau = \hat{R} - G\hat{\eta} \tag{5b}$$

The new independent variable τ, usually considered as a parameter along the characteristic line of the PDE (*6, 10*), is a combination of the time and x axes through velocity v. For the tubular reactor studied here, it has a physical significance explained in reference 5. By introducing a travelling time variable, the partial differential equations have been transformed into a set of ordinary differential equations. The variables $\hat{C}$ and $\hat{\eta}$ still refer to the given steady state profiles which are now functions of τ.

Because of the combination of independent variables,

the initial profiles in (1c) become transients of the transformed system and are therefore no longer explicitly needed in determining the dynamics of the transformed system. But since the inlet conditions in (1d) are needed as initial conditions in solving the transformed equations, these must be considered in the stability analysis of the transformed system. The initial conditions required by Equations (5) are

$$\hat{C}(\tau = 0) = \hat{C}_o; \ \hat{\eta}(\tau = 0) = \hat{\eta}_o \qquad (5c)$$

It should be noted that the suggestion of a transformation that substitutes an ordinary differential for a PDE is found in Zubov (*15*) and in Hahn (*6a*); however, these references deal with systems defined over an infinite interval. When these ideas were applied without modification to a PFTR they failed to give a region of stability or boundedness (*12a*). The approach is unnecessarily conservative, for it emerged from demands on an infinitely long reactor. It is certainly true that the stability of such an infinite system would guarantee the stability of any finite part of the reactor, but for engineering purposes, a more significant question applies specifically to the finite length, regardless of the ultimate behavior at infinite removal.

In effect Equations (4) and (5) offer two different ways to describe the transients of the same PFTR: one considers the transient distributions of the state variables along the whole reactor at any moment, and the other traces the transients of a whole set of fluid sections as they move along the reactor. The analysis that follows dwells primarily on the latter concept and takes Equations (5) as the transient equations of the PFTR system. However, the results will be interpreted both ways.

The transient equations of each fluid section are ordinary differential equations with time varying parameters: the steady state $[C_s(\tau), \eta_s(\tau)]$. The only effect of the time varying parameters on the transient equations is to shift the origin of the phase plane in such a way that it always corresponds to the steady state at any moment τ. The transients of each fluid section at any moment, $0 \leq \tau_j \leq \theta_L$, can be represented by a point in the CPP with the understanding that they refer to the steady state C_{sj} and η_{sj} at that specific moment.

As the fluid section moves along the reactor, its transients will trace on the CPP a trajectory unique to the initial conditions. Such a trajectory may appear on the CPP to be a loop, a contour crossing itself, or a simple point other than the origin. This peculiarity arises from the fact that the origin of the CPP corresponds to a pair of time varying parameters. A trajectory that appears to be a single point on the CPP implies that the transient profiles traced by a fluid section as it moves down the reactor runs parallel to the steady profile in $C - \eta - \tau$ space. A trajectory that crosses itself on the CPP means nothing more than that the differences $(\hat{C}, \hat{\eta})$ between the trajectory of the fluid section and the steady state profile at two or more instants τ_j are identical. Such characteristics on the CPP do not in any way indicate the nonuniqueness of the transient solutions of Equations (5). Some of the possible trajectories of a fluid section are shown in the composite phase plane of Figure 3.

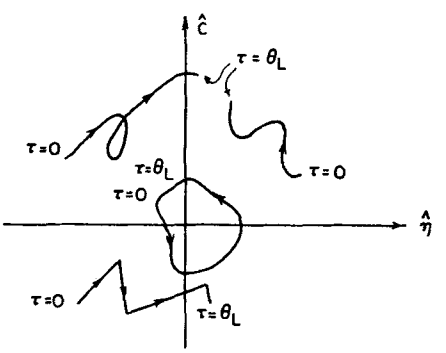

Fig. 3. Projections on the composite phase plane from trajectories traced by several fluid sections of a PFTR.

One can obtain the transient profile of a PFTR at any moment θ by proper combination of the trajectories of a series of fluid sections. It is instructive to study such combinations on the CPP to derive the equivalence between bounds on the trajectories and the confinement of the transient profiles. Assume that in Figure 4 curve *MN* indicates the continuous variations of the inlet condition of a PFTR from $\theta = \theta_M$ to $\theta = \theta_N$. From each point on *MN* a trajectory is traced by a small fluid section which is shown by the dashed line. These trajectories are all of finite length because the equal residence time of every fluid section is finite. Hence by collecting the terminal points of all trajectories we obtain the corresponding variations at the exit end of the reactor (line LP in Figure 4). At any time θ_j the transient curve can be formed by sequential combination of the transients of a series of consecutive fluid sections. Each trajectory in that series contributes one point in forming the instantaneous curve. By connecting these points on the CPP, one can obtain the projection of the transient curve at that moment, as is shown by a solid line in Figure 4. At each moment θ_j there is a projection of the instantaneous curve starting at a point of *MN* (the inlet condition) and ending at a point *LP* (the exit condition). A series of such solid lines between *MN* and *LP* indicate the time variations of the projection of the transient curve of the reactor from θ_M to θ_N.

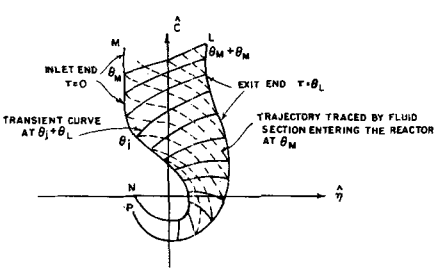

Fig. 4. Projections of transient curves of a PFTR through orderly combinations of the projections of trajectories of fluid sections.

These solid lines are not the same as the projected curves shown in Figure 2, differing in one important aspect. Having lost the identification of an x coordinate of the original transient curve, the projected curve does not correspond to a unique profile. On the contrary, though the solid lines in Figure 4 are also the projections of instantaneous curves, they were obtained through sequential combination of a series of trajectories of ordinary differential systems and correspond to unique transient curves. Such a sequential combination preserves both the direction (from inlet end to exit end) and the orderly position of the instantaneous curve along the x axis.

In Figure 4 the loci of inlet and exit disturbances are *MN* and *LP* in the time period $\theta_M \leq \theta \leq \theta_N$, and between *MN* and *LP* one can trace out the locus of instantaneous disturbances at any $\tau \leq \theta_L$ as the fluid section travels from inlet to outlet. Such constant τ loci are in

essence constant x loci. The solid lines between MN and LP are therefore projections that possess identifiable x positions of the transient curves of the reactor. Thus the dynamics of a PFTR system can be described by projections of instantaneous curves on the CPP between the loci of disturbances at inlet and exit (MN and LP).

The transient curve of a PFTR system always can be projected as one solid line between MN and LP, and conversely any solid line between MN and LP represents a unique transient profile of the system. Thus, a bound on one will limit the other.

Recall that initial conditions of a series of consecutive fluid plugs are the inlet conditions of the reactor for a period of time: $\theta_M \leq \theta \leq \theta_N$. Suppose that such inlet conditions are confined within a region δ in the $\hat{C} - \hat{\eta}$ plane at $\tau = 0$. Then by direct integration of Equations (5) a corresponding ϵ region can be obtained in the $\hat{C} - \hat{\eta}$ plane at $\tau = \theta_N$. Since the solutions of Equations (5) are uniquely determined by their initial conditions, the δ and ϵ regions are related by a point-to-point mapping, and if the inlet conditions of a PFTR are limited within a CPP region δ, the reactor exit conditions must lie in the CPP within a corresponding ϵ region. Moreover, because the transient curves generated from initial conditions within δ are confined within a CPP region between δ and ϵ, it is possible to find bounds to the transient curves.

CONSTRAINED INTEGRATION: THE ADIABATIC PFTR

When the PFTR system is adiabatic, the transient equations become symmetric and can be reduced to a one dependent variable system. To show that this is so, consider the adiabatic form of Equations (5):

$$D\hat{C}/D\tau = -\hat{R}(\hat{C}, \hat{\eta}; C_s, \eta_s) \tag{6}$$

$$D\hat{\eta}/D\tau = \hat{R}(\hat{C}, \hat{\eta}; C_s, \eta_s)$$

where $\hat{R}(\hat{C}, \hat{\eta}; C_s, \eta_s)$ indicates again that it is a function of $\hat{C}$ and $\hat{\eta}$ with two parameters C_s and η_s. By addition

$$D\hat{C}/D\tau + D\hat{\eta}/D\tau = D(\hat{C} + \hat{\eta})/D\tau = 0 \tag{7}$$

$$\hat{C} + \hat{\eta} = \hat{K} \tag{8}$$

From the end conditions at inlet

$$\hat{K} = \hat{C}_o + \hat{\eta}_o \tag{9}$$

that is, $\hat{K}$ is some constant which depends on the initial conditions of the fluid section. Equation (8) is equivalent to a constraint on the transients of an adiabatic PFTR, which arises from the symmetric form of the transient equations. A similar constraint was used in reference *14*. Since the steady state equations of such an adiabatic reactor are also symmetric, $K_s = C_s + \eta_s$ and $\hat{K}$ remains unchanged from inlet to exit within a given fluid section.

The constraint Equation (8) is represented by a family of straight lines on the CPP with slopes of -1 and intercepts of $\hat{K}$. These constraint lines are shown in Figure 5 for different values of $\hat{K}$. The transients of any fluid section must follow one of the straight lines. Once the initial disturbances of a fluid section fix $\hat{K}_i$, the transients of this fluid section will follow the particular constraint line $\hat{C} + \hat{\eta} = \hat{K}_i$ during its residence time in the reactor.

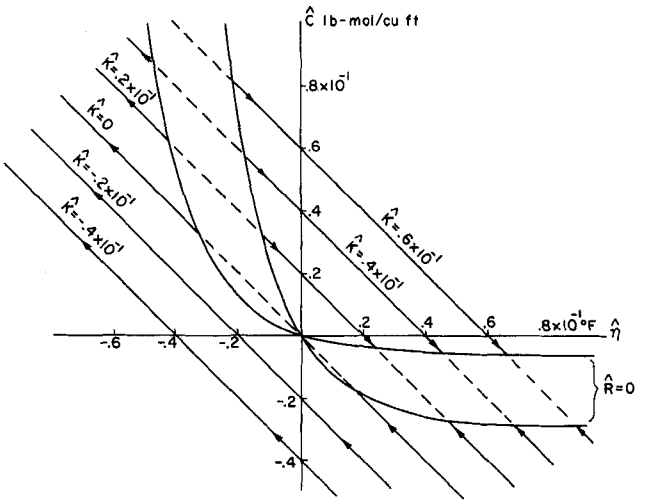

Fig. 5. The family of $\hat{R} = 0$ and straight line constraints of an adiabatic PFTR.

To estimate a region of stability it is necessary and desirable to take advantage of constraint Equation (8). By substituting Equation (8) into Equations (6) the original transient equations are changed into two separate, uncoupled equations:

$$D\hat{C}/D\tau = -\hat{R}_1(\hat{C}; \hat{K}, C_s, \eta_s) \tag{10a}$$

$$D\hat{\eta}/D\tau = \hat{R}_2(\hat{\eta}; \hat{K}, C_s, \eta_s) \tag{10b}$$

$\hat{R}_1$ and $\hat{R}_2$ are functions of $\hat{C}$ and $\hat{\eta}$, respectively, but both have three parameters K, C_s, and η_s. The solution of either (10*a*) or (10*b*) will give the whole transient picture of the system, for they are related through Equation (8). Equation (10*b*) gives the rate of temperature change along one of the constant $\hat{K}$ lines in the CPP. Its solution will measure how far the transient temperature will go along the constant $\hat{K}$ line from a given initial position $(\hat{\eta}_o, \hat{K})$. In general it is quite tedious to obtain regions of stability through integrations of transient equations, but for this particular case, because of constraint Equation (8), the simplicity of Equation (10*b*), and the convenient CPP, integration of Equation (10*b*) offers a direct way to find a region of stability.

In Figure 5 several constant $\hat{K}$ lines are drawn together with the extremes of the $\hat{R} = 0$ family for a particular steady state curve given. From Equation (6*b*) the sign of $\hat{R}$ is the same as that of $D\hat{\eta}/D\tau$. There are thus two regions in the CPP which are separated by the $\hat{R} = 0$ family, for which opposite signs of $D\hat{\eta}/D\tau$ will be found. At any point within the region $\hat{R} = 0$, $D\hat{\eta}/D\tau$ can be either positive, zero, or negative depending on which point (C_{sj}, η_{sj}) of the steady state curve it refers to. Combining the feature of constant K lines and regions of sign definiteness of $D\hat{\eta}/D\tau$, the tendency of transients of the system can be shown easily in the CPP. The arrows in Figure 5 indicate the tendencies of transients at different

sections of constant $\hat{K}$ lines. Anywhere to the left and below the $\hat{R} = 0$ family the movement is to decreasing $\hat{\eta}$ along 45 deg. lines, whereas anywhere to the right and above the $\hat{R} = 0$ family the movement is to increasing $\hat{\eta}$ along 45 deg. lines. Within the $\hat{R} = 0$ region the tendency can be either to increasing or decreasing $\hat{\eta}$, or $\hat{\eta}$ may remain stationary. This much information is sufficient to find a region of stability, for the object is not to pinpoint all the transient behavior of this system.

Assume for the moment that the critical bound on the transients is assigned at the exit end of the reactor as ϵ. For convenience ϵ may be chosen as a parallelogram about the origin of the CPP. To find the corresponding region δ at the inlet, a series of stage-by-stage, numerical integrations of Equation (10*b*) is carried out along some constant $\hat{K}$ lines that are within ϵ. Because ϵ is the given final bound ($\tau = \theta_L$) and δ is the limit at inlet ($\tau = 0$), the integrations are backward in the sense of moving time τ. Since the steady state curve is varying with respect to τ, the integration of (10*b*) from $\tau = \theta_L$ to $\tau = 0$ must be performed section by section.

Actual calculations are much simplified by the known transient tendencies shown in Figure 5. Only those $\hat{\eta}_o$'s along part of the boundary of region ϵ (that is, *AB* and *CD* in Figure 6) need be calculated, and it may be anticipated that the resulting δ should more or less look like the region *HIEFGH* enclosed by heavier lines. If the lower portion of δ, *HIDC*, can be neglected, calculations are necessary only along *AB*. The final δ region is *CDEFGC*. In this case only part of the boundary of δ (EFG) is obtained through numerical integrations; the other parts of the boundary are the results of straight line connections.

One may conclude that any disturbances at the inlet of the reactor which belong to δ should not get out of ϵ at the exit within the residence time of the fluid sections. Because the estimation of the δ region is made through continuous backward integrations with a given region ϵ from $\tau = \theta_L$ to $\tau = 0$, there should be an intermediate region δ_j at each τ_j, which corresponds to a unique pair of δ and ϵ. These δ_j's are defined along the reactor by Equation (10) such that in the process of finding δ the whole set of δ_j's from exit to inlet have been determined. The totality of δ_j's so calculated is a bounding region Ψ_τ in space $(\hat{C}, \hat{\eta}, \tau)$. Only the inlet and exit sections of Ψ_τ, δ and ϵ are shown in Figure 6. Since they are related through simple integrations along the constraint lines, the relationship between ϵ and δ is both sufficient and necessary: δ is implied by a given ϵ and vice versa. It is because of this unique correspondence that δ can sufficiently be determined by mapping through Equation (10) along only the boundary of ϵ.

In practical cases there are always some inequality constraints on state variables which ought to be considered in stability analysis. Suppose that simple constraints of the following forms are imposed on the PFTR system studied:

$$\underline{\hat{C}} < \hat{C} < \overline{\hat{C}} \qquad (11a)$$

$$\underline{\hat{\eta}} < \hat{\eta} < \overline{\hat{\eta}} \qquad (11b)$$

where $\overline{\hat{C}}$ and $\overline{\hat{\eta}}$ represent the upper and $\underline{\hat{C}}$ and $\underline{\hat{\eta}}$ the lower bounds on concentration and temperature disturbances. These bounds are not time (θ) dependent but may be space (x) dependent. For the moment they are assumed to be constant along the reactor. With reference to Figure 6 where a pair of δ and ϵ are shown, inequalities (11) are satisfied at every point within the rectangular region in the CPP.

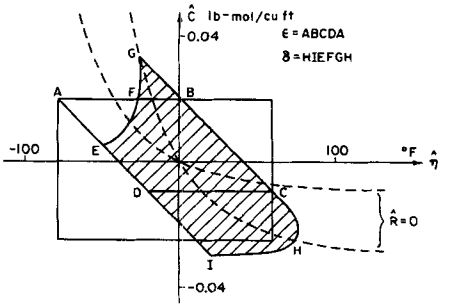

Fig. 6. The δ and ϵ regions of an adiabatic PFTR.

The common region between δ and the inequality constraint region on the CPP is defined as δ_m, the part of δ that is acceptable. Since δ_m is only a portion of δ, there is no longer the one-to-one correspondence between ϵ and δ_m. All possible transients with their initial disturbances belonging to δ_m will not at the exit occupy every part of ϵ. The trivial part of ϵ, where no transients from δ_m will reach, can be discarded without affecting the stability region of the system. In doing so the ϵ originally proposed is modified according to the practically acceptable δ_m. To find this modified ϵ from δ_m, forward integation as by (10) may be carried out along the boundary of δ_m. As a result a one-to-one correspondence is created between ϵ_m and δ_m, a pair shown in Figure 7. With all possible inlet disturbances inside δ, the transients of the system will be confined at exit within ϵ_m. In what follows a numerical example is worked out to show the feasibility of this approach with a set of realistic inequality constraints.

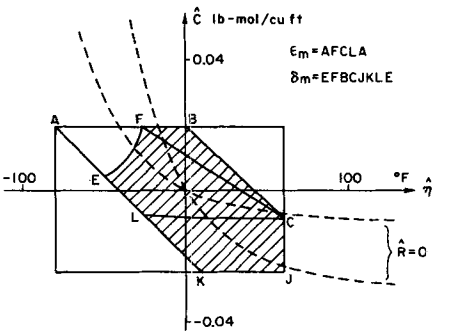

Fig. 7. The modified δ and ϵ of an adiabatic PFTR.

NUMERICAL EXAMPLE

A simple, irreversible, first-order exothermic reaction is assumed, with the kinetic rate of the Arrhenius type with respect to temperature: $CA \exp(-Q/T)$. System constants are chosen as follows:

$A = 1 \times 10^{10}$	liter/hr.
$Q = 9.4 \times 10^3$	B.t.u./°R.
$\Delta H = 1 \times 10^5$	B.t.u./lb.-mole
$\rho = 50$	lb.-mole/cu. ft.
$C_p = 1$	B.t.u./lb.-mole-°F.

$\overline{C} = 0.25$	lb.-mole/cu. ft.
$\overline{T} = 1{,}000$	°R.
$T_i = 580$	°R.
$C_i = 0.03$	lb.-mole/cu. ft.
$L = 5$	ft.

The steady state profiles from Equation (8) are shown in Figure 8. The corresponding $\hat{R} = 0$ family in the composite phase plane is shown in Figure 9. A rectangular region about the origin of the CPP is selected as the desirable region for the transients at the exit of the reactor, a choice consistent with the observation that only the upper and lower bounds of the state variables are specified. The region chosen for this example corresponds at the exit to a concentration change from 0.03 to −0.009 lb.-mole/cu. ft. (about 100% of inlet concentration) and a range of temperature change from 40° to −80°F. about the steady state.

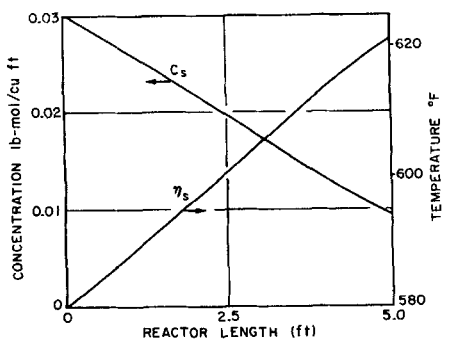

Fig. 8. Steady state profiles of an adiabatic PFTR.

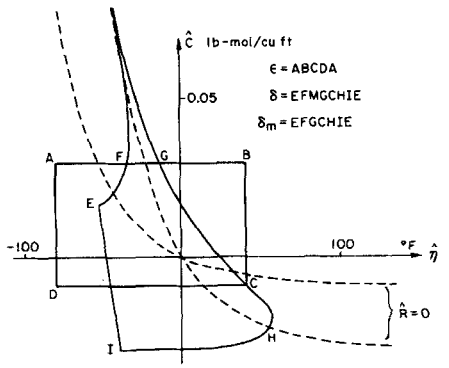

Fig. 9. The δ and ϵ of the example.

The state variable constraints arise from physical limitations on the system as follows:

$$0 < \hat{C} + C_s < \overline{C} \tag{12a}$$

$$\underline{\eta} < \hat{\eta} + \eta_s < \overline{\eta} \tag{12b}$$

$\overline{C}$ is the largest concentration anticipated or allowed; $\overline{\eta}$ and $\underline{\eta}$ are the largest and smallest temperatures specified or allowed for the reaction system, respectivly. $\overline{C}$, $\overline{\eta}$, and $\underline{\eta}$ are both time and space independent. Since C_s and η_s are profiles along the reactor, the constraints in (12) are therefore space dependent. After these inequalities are rearranged and put into discrete forms

$$-C_{sj} < \hat{C}_j < \overline{C} - C_{sj} \tag{13a}$$

$$\underline{\eta} - \eta_{sj} < \hat{\eta}_j \leq \overline{\eta} - \eta_{sj} \tag{13b}$$

where j is the index of increments along the τ axis. As shown in Figure 9, the constrained integrations outlined in the last section were carried out along the boundary of the ϵ region, namely, AB, BC, CD, and DA. Each integration step is checked by the inequality constraints (13).

The final results of these computations enable one to trace the δ_m region shown in Figure 9. Any disturbance in the fluid section at the inlet that is within the δ_m region will show transients bounded by the ϵ region when that fluid section reaches the exit end of the reactor. After δ_m has been found, the search for ϵ_m requires only forward integrations along the FG part of the boundary of δ_m. The resulting ϵ_m is shown in Figure 10. δ_m and ϵ_m having been found, the computations have already given the boundary surface of Ψ_τ in $(\hat{C}, \hat{\eta}, \tau)$ space. In Figure 10, the shaded area and portions of the straight line on the boundary are the projection of the boundary surface of Ψ_τ between its two ends. Once δ_m and ϵ_m are plotted on the CPP, one may get the picture of region Ψ_τ by inspection.

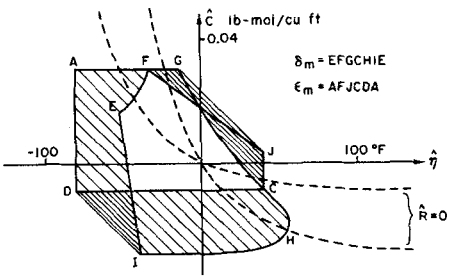

Fig. 10. ϵ_m and δ_m of the example.

Though the numerical example chosen shows rather straight steady state profiles in temperature and concentration (Figure 8), neither the procedures nor the results depend on this fact. That similar results were obtained for systems with more obviously curved profiles (*12a*) is perhaps not surprising in view of the fact that the steady states enter the analysis only as reference curves in the definitions prior to Equations (4).

NONADIABATIC PFTR

Since the system equations for a nonadiabatic PFTR are not symmetric, the procedure is somewhat different from that for the adiabatic PFTR; nevertheless, bounds on the transients of a nonadiabatic PFTR with two state variables $(\hat{C}, \hat{\eta})$ can be found with virtually no more effort than is required by the adiabatic case. In the following a graphical composite phase plane approach is developed to estimate a region of practical stability for any steady state profile of a PFTR system with respect to excursions of the most common variety. The tracking function (9) and isocline (12) methods are exploited.

Define W by

$$W_s = C_s + \eta_s \tag{14a}$$

$$\hat{W} = \hat{C} + \hat{\eta} \tag{14b}$$

Then, combining Equations (5a) and (5b) one obtains

$$D\hat{W}/D\tau = G\hat{\eta} \qquad (15)$$

Equations (5a) and (15) may be used to restrict the slopes of transients at different regions in the CPP, since they determine the trajectories' directions with respect to $\hat{C}$ and $\hat{W}$ as functions of $\hat{R}$ and $\hat{\eta}$, respectively. That is, transients must move in the direction of decreasing $\hat{C}$ in any region of the CPP in which $\hat{R} > 0$; they must move in the direction of decreasing $\hat{W}$ in the right half plane where $\hat{\eta} > 0$. These and similar restrictions for other regions are summarized in Table 1 and by the arrow symbols in Figure 11. The family of $\hat{R} = 0$ for a given steady state profile is also shown by the two extreme curves among the family, and the $\hat{W}$ axis is shown as the straight line passing through the origin with a 45 deg. slope. A point in the region occupied by the $\hat{R} = 0$ family may have a positive, zero, or negative $D\hat{C}/D\tau$, depending on which single curve $\hat{R}_j = 0$ it refers to. In the terminology of reference 9, $\hat{W}$ and $\hat{C}$ may be considered as tracking functions in the CPP, but it is worth noting that $\hat{W}$ is a special tracking function: it is independent of the steady state profile, since the $\hat{C}$ axis is the only curve in the CPP that separates a region of $D\hat{W}/D\tau < 0$ from one where $D\hat{W}/D\tau > 0$.

With this information about the slopes and tendencies of transients on hand, it is possible to draw lines which confine the transients in most of the regions itemized in Table 1. With reference to Figure 12, a straight line with -1 slope bounds all transients below it in regions A and H. Likewise, in regions D and F a straight line with -1 slope limits all transients above it. A horizontal line will confine the transients above it in region B and below it in region E. By connecting these bounding lines as shown, an almost enclosed region is formed about the origin, open only in regions D and F. If, as is often the case, a designer is concerned only with possible excursions in the direction of temperature increase (runaways, hotspots), these bounds can be a practically reasonable basis for design. If, on the other hand, there is danger in the low temperature, high concentration direction, a means must be found to close the gap in regions D and F. A technique for this will be explored in a following paper.

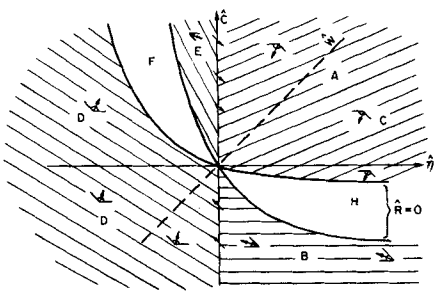

Fig. 11. The tendencies of trajectories traced by fluid sections of a nonadiabatic PFTR.

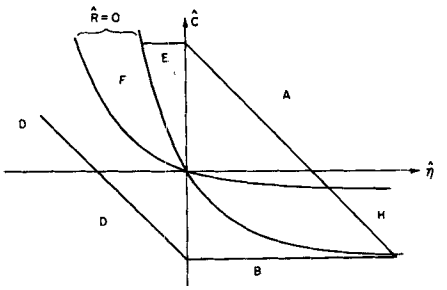

Fig. 12. An almost closed parallelogram on the CPP formed by bounding straight lines.

TABLE 1. QUALITATIVE DESCRIPTION OF THE TRANSIENTS $(\hat{C}, \hat{\eta})$ ON THE CPP FOR THE NONADIABATIC PFTR

Region or line	Constraints from Equations (5a) and (15)	Slope $= \dfrac{d\hat{C}}{d\hat{\eta}}$	Trends of trajectory
Positive $\hat{C}$ axis	$D\hat{C}/D\tau < 0$	-1	To decrease $\hat{C}$
	$D\hat{\eta}/D\tau > 0$		To increase $\hat{\eta}$
Negative $\hat{C}$ axis	$D\hat{C}/D\tau > 0$	-1	To increase $\hat{C}$
	$D\hat{\eta}/D\tau < 0$		To decrease $\hat{\eta}$
A	$D\hat{C}/D\tau \leq 0$	-180 deg. $\leq \phi \leq -45$ deg.	To decrease $\hat{C}$
	$D\hat{W}/D\tau \leq 0$		To decrease $\hat{W}$
B	$D\hat{C}/D\tau \geq 0$	135 deg. $\leq \phi \leq 180$ deg.	To increase $\hat{C}$
	$D\hat{W}/D\tau \leq 0$		To decrease $\hat{W}$
D	$D\hat{C}/D\tau \geq 0$	0 deg. $\leq \phi \leq 135$ deg.	To increase $\hat{C}$
	$D\hat{W}/D\tau \geq 0$		To increase $\hat{W}$
E	$D\hat{C}/D\tau \leq 0$	-45 deg. $\leq \phi \leq 0$ deg.	To decrease $\hat{C}$
	$D\hat{W}/D\tau \geq 0$		To increase $\hat{W}$
F	Similar to the case in either region D or region E		
H	Similar to the case in either region A or region B		

DISCUSSION

The composite phase plane approach is limited to systems with one physical dimension. In the foregoing it was applied to the PFTR, but it is still valid in the presence of axial mixing. This extension is the subject of another paper now in preparation; however, it may be pointed out that in this case the simple PFTR relations between transient bounds and their projections on the CPP are lost. If, on the other hand, the distributions of temperature and concentration in both axial and radial directions of a tubular reactor are considered, the system has two physical dimensions, and projections in the x direction alone will fail to describe the dynamics of such a system.

Such a limitation in dimensionality does not occur in principle with regard to the dependent variables, and it is conceptually possible to study systems with three or more state variables by projecting along the steady state profile. Such studies would, however, be seriously hampered by the difficulties and limitations common to higher dimensional state space graphs: primarily those arising from the multidimensional visualizations which are demanded. For practical engineering analysis, this technique seems in effect to be applicable only to systems with one physical dimension and two state variables, well suited to many tubular reactor studies.

Another phase plane analysis (*1, 3*) may be cited for the sake of comparison and to further illustrate the CPP. Eliminating the time variable from Equations (5), but not using deviation variables, one can obtain

$$\frac{D\eta}{DC} = -1 + G\frac{(\eta - \eta_w)}{R} \qquad (16)$$

an equation representing the differential relation between C and η at any τ (or x). With a pair of C and η known at inlet, the solution of Equation (16) traces the concentration and temperature of a fluid section as it flows through the reactor. Such a solution can be represented as a curve on the $C - \eta$ plane which is called a *reaction path* in reference *1*. This reaction path is in essence the projection on the $C - \eta$ plane of a trajectory of any fluid section in the space (C, η, τ). In a similar manner, if Equation (3*b*) is combined with Equation (3*a*), one obtains

$$\frac{d\eta_s}{dC_s} = -1 + G\frac{(\eta_s - \eta_w)}{R_s} \qquad (17)$$

This equation, a special case of the previous one, is used in reference 3 to show the reaction path of any fluid section for a pair of inlet conditions fixed in time θ. The resulting curve on the $C - \eta$ plane is also the projection of the steady state curve in space (C, η, x). This phase plane differs from the composite phase plane in one aspect: the origin of the CPP corresponds to the steady state curve, while the $C - \eta$ plane has an origin at a pair of fixed values of C and η. Thus the reaction path shown in reference 3 has shrunk to a single point at the origin of the CPP. This further makes clear that the CPP has to be expressed in terms of disturbance variables $(\hat{C}, \hat{\eta})$, and it cannot be converted back to the $C - \eta$ plane by simple translation of coordinates as is the case for the ordinary phase plane for lumped parameter systems.

ACKNOWLEDGMENT

This research was supported by a grant from the National Science Foundation.

NOTATION

A = frequency factor
A_r = heat transfer area per unit volume of reactor
C = concentration of reactant
C_p = specific heat
G = normalized heat of reaction
ΔH = molal heat reaction
K = overall heat transfer coefficient; constraint constant
L = length of a reactor
R = rate of chemical reaction
T = absolute temperature
v = velocity of fluid or flow rate in the reactor
W = combined variable defined by Equation (16)
x = reactor length dimension

Greek Letters

δ = region in the state space (or CPP) which corresponds to the inlet end of the reactor
ϵ = region in the state space (or CPP) which corresponds to the exit end of the reactor
η = normalized temperature, $\left(\frac{TC_p\rho}{\Delta H}\right)$
θ = time
ρ = density
τ = moving time variable
Ψ_τ = bounding region

Superscript

$\wedge$ = disturbance variable

Subscripts

i = initial condition
o = inlet condition
s = steady state
L = at exit

LITERATURE CITED

1. Aris, Rutherford, "Introduction to the Analysis of Chemical Reactors, "Prentice-Hall, Englewood Cliffs, N. J. (1965).
2. ———, and N. R. Amundson, Chem. Eng. Sci., 7, 121 (1958).
3. Barkelew, C. H., *Chem. Eng. Progr. Symp. Ser. No. 25*, **55**, 37 (1959).
4. Berger, J. S., and D. D. Perlmutter, *AIChE J.*, **10**, 233 (1964).
5. Bird, R. B., W. E. Stewart, and E. N. Lightfoot, "Transport Phenomena," Wiley, New York (1960).
6. Courant, R., and D. Hilbert, "Methods of Mathematical Physics," Vol. 2, Interscience, New York (1962).

6*a*. Hahn, Wolfgang, "Theory and Application of Liapunov's Direct Method," p. 137, Prentice-Hall, Englewood Cliffs, N. J. (1963).

7. Leathrum, J. F., E. F. Johnson, and Leon Lapidus, *AIChE J.*, **10**, 16 (1964).
8. Luyben, W. L., *ibid.*, **12**, 662 (1966).
9. Paradis, W. O., and D. D. Perlmutter, *ibid.*, 130.
10. Reilly, M. J., and R. A. Schmitz, *ibid.*, 153.
11. Schmitz, R. A., and N. R. Amundson, *Chem. Eng. Sci.*, **18**, 391 (1963).
12. Truxal, J. G., "Automatic Feedback Control Systems Synthesis," McGraw-Hill, New York (1960).

12*a*. Wang, F. S., Ph.D. thesis, Univ. Illinois, Urbana (1966).

13. Warden, R.B., Rutherford Aris, and N. R. Amundson, *Chem. Eng. Sci.*, **19**, 149, 173 (1964).
14. Wei, James, *ibid.*, **20**, 729 (1965).
15. Zubov, V. I., "Methods of A. M. Lyapunov and Their Application," Leningrad (1957); available as AEC Translation 4439 (1961).

Manuscript received December 16, 1966; revision received May 31, 1967; paper accepted June 5, 1967. Paper presented at AIChE Houston meeting.